NASA Technical Memorandum 101448

Low Frequency Vibration Isolation Technology for Microgravity Space Experiments

Carlos M. Grodsinsky and Gerald V. Brown
Lewis Research Center
Cleveland, Ohio

Prepared for the
12th Biennial Conference on Mechanical Vibration and Noise
sponsored by the American Society of Mechanical Engineers
Montreal, Canada, September 17–20, 1989

NASA

LOW FREQUENCY VIBRATION ISOLATION TECHNOLOGY FOR MICROGRAVITY SPACE EXPERIMENTS

Carlos M. Grodsinsky and Gerald V. Brown
National Aeronautics and Space Administration
Lewis Research Center
Cleveland, Ohio 44135

SUMMARY

The dynamic acceleration environment observed on Space Shuttle flights to date and predicted for the Space Station has complicated the analysis of prior microgravity experiments and prompted concern for the viability of proposed space experiments requiring long-term, low-g environments. Isolation systems capable of providing significant improvements in this environment exist, but have not been demonstrated in flight configurations. This paper presents a summary of the theoretical evaluation for two one degree-of-freedom (DOF) active magnetic isolators and their predicted response to both direct and base excitations, that can be used to isolate acceleration sensitive microgravity space experiments.

NOMENCLATURE

C	capacitance
c	electro-magnet damping coefficient
F_S	isolator force
g_0	acceleration of the Earth at the surface
I_{avv}	electro-magnet current (α velocity)
i_b	magnetic-circuit current bias
K	passive stiffness coefficient
k_a	magnetic-circuit current amplifier stiffness
k_{eq}	magnetic-circuit isolator stiffness
k_g	magnetic-circuit proportional gain
k_i	magnetic-circuit current stiffness
k_p	magnetic-circuit sensor amplifier gain
k_r	magnetic-circuit derivative gain
k_θ	magnetic-circuit position stiffness
m	mass
N	number of ampere turns
R	resistance
u	position of base
x	position of payload
ξ_1	passive damping coefficient
τ	time constant = RC
ψ	magnetic field strength
ω	excitation frequency
ω_{na}	active system resonance frequency
ω_n	system resonance frequency

INTRODUCTION

Interest in vibration isolation for microgravity experiments has increased within the microgravity science community as the flight program has progressed and the small, but significant levels of residual acceleration on the Space Shuttle (STS) have become more widely recognized and documented (Hamacher, 1986: Workshop Proceedings, 1986). These background accelerations result from several sources characteristic of the orbiting carrier and the orbital environment. Very low frequency (10^{-3} Hz to dc) accelerations due to drag, tidal effects, and gravity gradients contribute submicro-g/g_o levels. STS thruster activity can contribute 10^{-4} to 10^{-2} g/g_o accelerations with significant duration, but can be predicted and controlled. The most visible and troublesome contribution to most experiments is the moderate frequency (10^{-3} to 100 Hz) dynamic spectrum of accelerations having magnitudes in the range 10^{-5} to 10^{-2} g/g_o. This dynamic background is due substantially

to random excitations from manned activity on the orbiter. However, orbiter structure and flight systems also contribute observable intermittent and resonant accelerations to the background as the orbiter interacts with its dynamic mechanical and thermal environment.

The evolution of the Space Station design has led to many discussions of the potential limitations on long term, low gravity experimentation in this environment. It is now obvious that most of the true microgravity experiments will require "protection" from this random, milli-g environment if valid and reproducible results are to be expected. Because a large part of the transient disturbances have a frequency range from milli-Hz to 1 Hz, it is extremely difficult to design a passive isolation system with a resonance frequency at most $1/\sqrt{2}$ times the lowest excitation frequency of interest, mainly the sub-Hz range.

The serious limitation of passive isolators is the absence of materials which have useful ranges of both low-modulus (providing low frequency) and appropriate damping (to avoid large amplitude oscillation). Two-stage passive isolators can decrease the frequency but limited damping leads to potentially unstable systems in the random excitation environment. It is apparent that a passive isolation system would not suffice because of the requirement of an extremely low stiffness for the isolation of small disturbance frequencies for typical values of mass for microgravity experiments. On the other hand, when there are direct disturbances on the payload, a small value of stiffness is not desirable. Therefore, there is a trade off, and an optimal design would need to compensate for both direct disturbances, if present, and low frequency base disturbances. Thus, active systems offer significant advantages over passive systems in the orbital acceleration environment, due to both the extremely small stiffnesses needed to isolate against such low frequency base disturbances and the ability to adapt to direct disturbances for the optimal isolation of the payload, since the responses to these two excitations require conflicting solutions.

Active systems require sensing of motion or position and a feedback control loop to counteract mechanical excitation and minimize motion of an isolated body. Such systems introduce the complexity of a high-gain control system, but offer significant advantages in versatility and performance (Ruzicka, 1969).

This paper summarizes the theoretical evaluation of both a fully magnetically suspended one DOF system and a passive static support system but with electromagnetic damping. The fully magnetically suspended system is evaluated using an attractive electromagnet, while the electromagnetically damped system is evaluated using a Lorentz magnet. These magnetic systems, specifically the attractive type, have been used for the suspension of rotating shafts for a number of years and the required negative feedback loops to control such systems have been discussed in numerous papers, giving the equivalent stiffness and damping coefficients for specific controllers. However, these studies have not been interested in the isolation of the suspended body from direct and base excitations. Thus, the response of such systems to these type of disturbances has not been documented. Therefore, we evaluate the dynamic response to base and direct disturbances of both systems. A pictorial representation of both systems evaluated is shown in Fig. 1 where both systems can be represented by an isolator between a base support and the isolated payload. This isolater is simply an actuator which is driven in proportion to certain feedback signals depending on a desired response of the payload. Specifically, for the magnetic-circuit isolator, an attractive magnetic actuator was analyzed where both

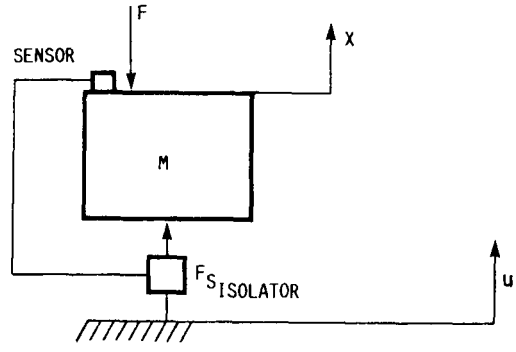

FIGURE 1.

the stiffness and damping coefficients are derived from a relative position sensor and for the electromagnetic damping isolator a Lorentz actuator was analyzed where the damping coefficient was derived from an inertial sensor and the stiffness of the isolator is simply a constant spring stiffness of a passive spring. Presently, there are laboratory models of these theoretically represented one DOF isolation systems. However, the emphasis at NASA Lewis is to perform digital active control on dependent multidegrees of freedom. Currently, these systems are projected for test in a full six DOF free fall condition, provided by the NASA Lewis low gravity aircraft, in order to acquire the coupled response between all six DOF in a low gravity environment.

STATEMENT OF THE PROBLEM

To categorize the disturbances which are present in the Space Shuttle and will be present in the Space Station, one can group these accelerations into three frequency ranges (Jones et al., 1987):

(1) Quasi-Static External Disturbances
(2) Low Frequency Vibration Sources
(3) Medium-High Frequency Vibrations

The disturbances listed under the first category are aerodynamic drag, gravity gradient effects and photon pressure accelerations. These accelerations have frequency ranges less than a mHz and acceleration magnitudes of about 10^{-7} g/g_o and lower. The second catagory would include excitations due to large flexible space structures, crew motion, spacecraft attitude control, and robotic arms. These disturbances range from mHz to about the 10 Hz frequency range. The third catagory would list disturbances due to on-board equipment such as pumps and motors having a dynamic range of about 10 Hz and above. (See appendix (Hamacher, 1986; Ruzicka, 1969; Hamacher et al., 1986).)

OVERVIEW

The active isolators described in this paper are effective at a frequency range of about a tenth of a Hz and above. This constraint does not arise from a technology limitation, but from practical limitations due to the fact that the strokes needed to isolate against the very low frequency range are not obtainable because of the volume constraints in the shuttle and in the future Space Station manned environment laboratory modules. For example, aerodynamic drag is a function of the atmospheric conditions during a specific mission, but an average magnitude of 10^{-7} g/g_o will be used for the sake of argument. Therefore, the frequency at which such a disturbance would act, in a

solar pointing station, would be at the orbital frequency, which is about 90 min per orbit. Thus, the distance an object would travel under such an acceleration would be $x = (a/\omega^2)2 = 1.5$ m (4.7 ft), not including initial conditions. Thus, realistically, an isolated payload would have to follow such movement of the spacecraft and be active in a much smaller region, which would depend on volume constraints of a payload in the shuttle or Space Station microgravity modules.

The following two cases can be analyzed as spring-mass damper systems, where the spring and damper characteristics are actively controlled and translated into actuator response by a control law depending on the response characteristics desired. Using an attractive electromagnet actuator, one can produce forces in only one direction. Therefore, to achieve a push-pull configuration one needs to use two electromagnets acting on an armature. For these electromagnet actuators, the force produced by one magnet is proportional to the square of the current and inversely proportional to the square of the gap, making the system open loop unstable. Due to these nonlinear characteristics, a bias current linearization technique is utilized. In addition, nonlinearities also arise between magnetic flux and input coil current due to hysteresis and saturation. In order to control this system, one must close a control loop around position and velocity feedback signals with a bias current to work in the more linear regime of the force versus current plot of a magnetic-circuit as shown in Fig. 2.

Figure 2 shows the magnetic-circuit actuator's squared dependence on current. Thus, the current bias i_b is used to produce a nearly linear control law such that for small disturbances about this current the control force produced can be assumed linear.

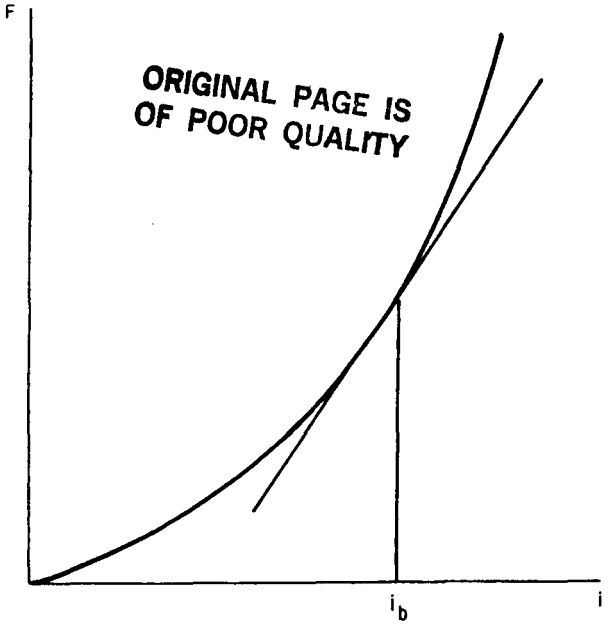

FIGURE 2.

In contrast, the Lorentz actuator can produce forces bidirectionally. The force produced by a Lorentz actuator is a vector quantity equal to the current cross field, ψ. Therefore, depending on the direction of current flow in the coil one can produce a force in either a positive or negative direction. Due to this actuator's linear dependence with the control current and because it is not simply an attractive system, the control law for this actuator is open loop stable. The Lorentz actuator, being a linear device, has advantages over the magnetic-circuit, but the power needed to produce a certain force is higher for a Lorentz actuator than for an attractive magnetic-circuit configuration. However, due to the small forces needed to control a payload in the weightless environment of space, this inefficiency is not as limiting as in the earth's gravitational field.

The basic concept behind these active isolation techniques is the sensing of position, velocity and/or acceleration, and driving an actuator 180° out of phase with this signal in order to cancel a disturbance to the payload. If there is some knowledge about certain disturbances, a feed forward loop could also be employed to anticipate an excitation and react to it without an error signal. These active isolation techniques can be implemented using either analog or digital control schemes to close the feedback or feed forward control loops.

To summarize the linearized control law for a one DOF magnetic-circuit isolator and the linear control law for a Lorentz electromagnetically damped one DOF system, one can give their transmissibilities and effectiveness in isolating against both base and direct disturbances. First, the response or transmissibilities of both systems will be generated for harmonic base excitations, using the active isolation system's differential equations of motion. These equations of motion were written using Newton's first and second laws. Where u is actually a time function so $u = u(t)$ with the same implied for a directly applied force, such that in actuality $F = F(t)$. Therefore, for a spring mass damper system, the equations of motion for base excitation become:

Magnetic-circuit Isolator

$$m\frac{d^2x}{dt^2} + k_{eq}(x - u) + c_{eq}\left(\frac{dx}{dt} - \frac{du}{dt}\right) = 0 \qquad (1)$$

Electromagnetic damping Isolator

$$m\frac{d^2x}{dt^2} + c\frac{dx}{dt} + Kx = Ku \qquad (2)$$

These systems look very similar to passive viscoelastic systems with the exception that, for all practical purposes, the stiffness and damping of both the magnetically suspended isolator and the electromagnetic damping case can be set at whatever coefficient is desired for an appropriate response to an excitation source. Therefore, these systems can be easily configured for an adaptive system where, by using sensed information from the disturbance environment, the control law could be changed to optimize the isolation of the payload. In using the magnetic-circuit actuator as an isolator, the stiffness and damping are not purely independent. However, this dependency is minimal and if certain control parameters are not violated, these isolation parameters can be assumed to be independent. To achieve a purely damped response independent of stiffness, be it active or passive stiffness, one would need to use a Lorentz actuator. In contrast, for the magnetic-circuit case, a certain amount of damping is needed in order to overcome open loop instability.

In defining the dynamic base motion equations for both systems, the stiffness and damping terms can be solved by using the appropriate control law needed for a stable negative feedback system. In summary, the stiffness coefficient for the magnetic-circuit becomes:

$$k_{eq} = k_\theta + \frac{k_i k_a k_p\left[k_g\left(1 - RC\tau_1\omega^2\right) + (k_g + k_r)(RC + \tau_1)RC\omega^2\right]}{\left(1 - RC\tau_1\omega^2\right)^2 + (RC + \tau_1)^2\omega^2} \quad (3)$$

and for the electromagnetic isolator, because the mass is being statically supported by a passive spring, the stiffness is simply K. Summarizing the damping coefficients for both isolators, the magnetic-circuit damping coefficient becomes:

$$c_{eq} = \frac{k_i k_a k_p\left[\left(1 - RC\tau_1\omega^2\right)(k_g + k_r)RC - k_g(RC + \tau_1)\right]}{\left(1 - RC\tau_1\omega^2\right)^2 + \left(RC + \tau_1\right)^2\omega^2} \quad (4)$$

and for the electromagnetic damping case:

$$c = -\psi N I_{avv} \quad \text{where:} \quad I_{avv} = E_{avv}/R \quad (5)$$

(Note: calculations assume negligible inductance)

As one can see, the magnetic-circuit actuator system is more complex than the Lorentz actuator due to the nonlinear characteristics of the magnet. Also, since the stiffness is a function of the excitation frequency, the natural frequency of this system is not constant. However, for small excitation frequencies, which is the range of interest, the natural frequency of the system can be assumed constant. The stiffness and damping solutions for both cases are summarized in a paper which is in preparation (Grodsinsky, 1989). However, the stiffness and damping coefficients for the magnetic-circuit isolator case are derived in a manner similar to those which arise for a magnetic bearing configuration, and such derivations can be found in many papers on the subject of magnetic bearings; for example (Humphris, 1986).

In order to solve the equations by defining the base excited system transfer function, the dynamic equations will be transformed into the frequency domain using the Laplace transformation:

$$F(s) = \int_{-\infty}^{\infty} F(t)e^{-st}dt \quad (6)$$

Then, transforming the transfer functions into vibration notation, the two equations become:

Magnetic-circuit Transfer Function

$$\frac{X}{U}(s) = \frac{2\xi\omega_n s + \omega_n^2}{s^2 + 2\xi\omega_n s + \omega_n^2} \quad (7)$$

Electromagnetic Damping Transfer Function

$$\frac{X}{U}(s) = \frac{\omega_n^2}{s^2 + 2\xi\omega_n s^2 + \omega_n^2} \quad (8)$$

Thus, the frequency response for both functions are obtained by the relation:

$$\frac{X}{U}(j\omega) = \lim_{t\to\infty}\left[\frac{X}{U}(s)\right] \text{ for } s = j\omega \quad (9)$$

where: $j = \sqrt{-1}$

Thus, the transfer functions in terms of frequency response are vectors in the complex plane and the magnitudes of vibrations measured on the isolated payload resulting from a sinusoidal excitation usin(ωt) is the vector length of $X/U(j\omega)$. This value is a scalar, since the phase angle is not used, and is called the transmissibility function of the system. The transmissibility is generally written as $T = |X/U(j\omega)|$.

Therefore, the transmissibility functions for both systems of interest become:

Magnetic-circuit Transmissibility Function

$$T = \left|\frac{X}{U}(j\omega)\right| = \sqrt{\frac{1 + \left[2\xi\frac{\omega}{\omega_n}\right]^2}{\left[1 - \left[\frac{\omega}{\omega_n}\right]^2\right]^2 + \left[2\xi\frac{\omega}{\omega_n}\right]^2}} \quad (10)$$

Electromagnetic Damping Transmissibility Function

$$T_{av} = \left|\frac{X}{U}_{av}(j\omega)\right| = \sqrt{\frac{1}{\left[1 - \left[\frac{\omega}{\omega_n}\right]^2\right]^2 + \left[2\xi\frac{\omega}{\omega_n}\right]^2}} \quad (11)$$

By plotting these transmissibilities, one can see the effect of changing the stiffness or damping of either system. As can be seen from the stiffness coefficient for the magnetic suspension case, using the attractive magnetic-circuit actuator, the natural frequency of the system is frequency dependent on the excitation source. However, for small disturbance frequencies of 100 Hz and below, this dependence is negligible and ω_n is assumed constant. The transmissibility curve for the first case is illustrated in Fig. 3. Figure 3 demonstrates the effect of increasing the damping coefficient of the magnetic-circuit isolator system. As can be seen by the curves in Fig. 3, increasing the velocity feedback gain, K_r, the system can become overly damped, which gives rise to the damped response at resonance and less isolation at excitation frequencies above $\sqrt{2}$ times ω_n than would be achievable with a less damped system. The effect of increasing the position gain would shift the natural frequency of the system to the right because of the increase in equivalent stiffness of the system, while the opposite would result by decreasing the position gain K_g. The subsequent electromagnetic damping case is illustrated in Fig. 4. Figure 4 shows the effect of increasing the damping coefficient of the Lorentz electromagnetic damping system. The curves show the response of the system to increasing the velocity feedback term and thus, increasing the damped response of the system. The advantage of active damping feedback, derived from an inertial reference, is that it can remove the resonant response, broadening and smoothing the transition between the low frequency and high frequency regions, while reducing both the transmission and the response, particularly in the low frequency range of interest. The effects of such a system for large values of velocity feedback gain can be understood by considering that it is equivalent to having a passive damper attached between the isolated mass and a virtual inertial reference. As the friction in the damper is increased, the isolated mass becomes more and more tightly coupled to the (motionless) ideal inertial reference. Unlike the passive

damper, the stronger the coupling, the better the isolation. This arises because the velocity proportional gain is determined from the integration of an inertial sensor signal. This type of response is not seen in the pure suspension case because the velocity term was determined from the derivative of a relative position sensor giving rise to the response shown in Fig. 3.

$$\xi = \frac{K_i K_g K_p [K_g + K_r) - K_g 1.022] 10^{-3}}{(1 - RC\omega^2)^2 + (RC + \tau_1)^2\omega^2}$$

$$\omega_n^2 = K_\theta + \frac{K_i K_g K_p [K_g(1 - RC\tau_1\omega^2) + (K_g + K_r)(RC + \tau_1)RC\omega^2]}{(1 - RC\omega^2)^2 + (RC + \tau_1)^2\omega^2}$$

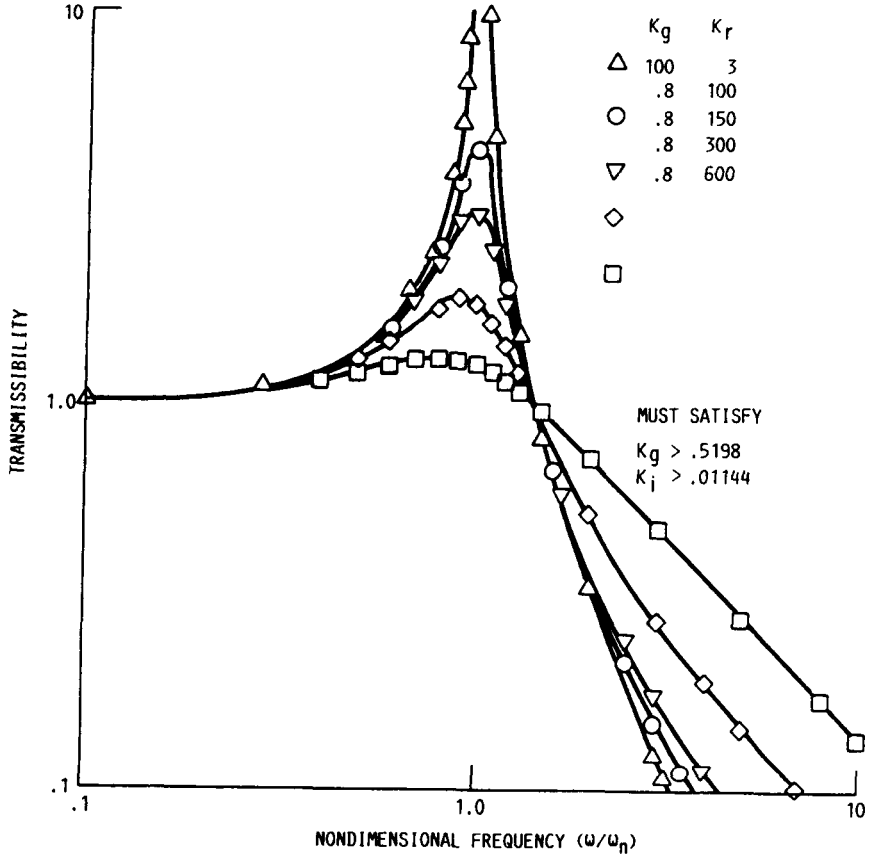

FIGURE 3.

In order to relate these curves to the microgravity environment, one can use a g/g_o versus frequency plot, which was generated from typical Microgravity Science Laboratory acceleration data (refs. 1 and 2), and superimpose these transmissibility curves on this data, to predict the isolation performance achievable for such disturbances, measured on an earlier shuttle flight. By superimposing these curves, one can get a rough idea of the capability of such techniques in isolating against such low frequency disturbances. These curves are presented in Fig. 5 (Hamacher, 1989; Ruzicka, 1969). Figure 5 shows selected peak accelerations (open data points) typical of those observed on STS missions (Hamacher, 1989; Ruzicka, 1969) and an upperbound (line with positive slope) that is intended to reflect the "worst case" limit for a transmissibility curve of a theoretical isolator. The filled data points show the effect of filtering this "mechanical noise" through such an isolator and the resultant "worst case" line.

As explained previously, these curves all demonstrate system response to base excited harmonic motions. However, disturbances may also be generated directly on the payload itself. The sensitivity of the isolated payload to a disturbing force will be characterized by a term called the isolated payload mobility. The mobility of the payload is the vector magnitude of $X(s)/F(s)$. This parameter measures the amplitude of the payload deflection per unit of force amplitude. The equations of motion for both systems, for direct disturbance only are:

Magnetic-circuit Equation of Motion

$$M\frac{d^2x}{dt^2} = F(t) - K_{eq} - C_{eq}\frac{dx}{dt} \qquad (12)$$

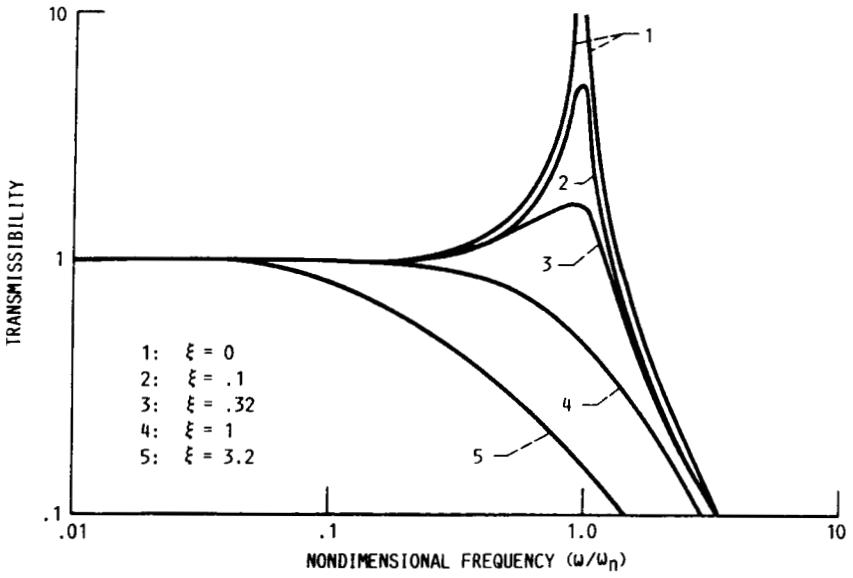

FIGURE 4.

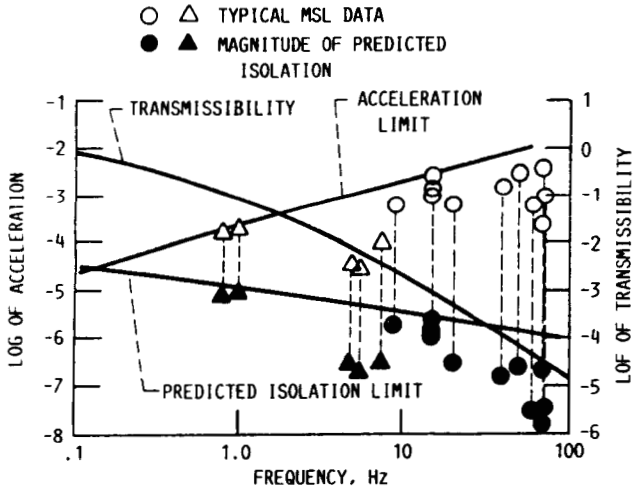

FIGURE 5.

Electromagnetic Damping Equation of Motion

$$M\frac{d^2x}{dt^2} = F(t) - Kx - c\frac{dx}{dt} \qquad (13)$$

These equations can be placed in the Laplace operation format and from the definition of the vector magnitude X(s)/F(s), one can write the mobility equation for both cases as follows:

Magnetic-circuit Mobility Equation

$$\frac{X(s)}{F(s)} = \frac{1}{Ms^2 + C_{eq}s + K_{eq}} \qquad (14)$$

Electromagnetic Damping Mobility Equation

$$\frac{X(s)}{F(s)} = \frac{1}{Ms^2 + cs + K} \qquad (15)$$

In order to evaluate the effectiveness of these active systems, the ratio of X(s)/F(s) active to X(s)/F(s) for an equivalent passive system will be used. This ratio will be called the mobility effectiveness $X_f(s)$. Therefore, if $X_f(s)$ is unity, the active system does nothing. If $X_f(s)$ is zero, no motion of the payload results from a finite applied force. If $X_f(s)$ is greater than unity, then the active system amplifies the effect of the applied force, increasing the payload motion. The equations for the effectiveness function for both cases, in terms of frequency response, where the vector length of $X_f(s)$ is $|X_f(j\omega)|$, become:

Magnetic Circuit Effectiveness

$$\left|X_f\left[\frac{j\omega}{\omega_n}\right]\right| = \frac{\omega_n}{\omega_{na}}\sqrt{\frac{\left[1-\left[\frac{\omega}{\omega_n}\right]^2\right]^2 + \left[2\xi_1\frac{\omega}{\omega_n}\right]^2}{\left[1-\left[\frac{\omega}{\omega_n}\right]_a^2\right]^2 + \left[2\xi\frac{\omega}{\omega_n}\right]_a^2}} \qquad (16)$$

Where: for small excitation frequencies $\omega_{na} \approx \omega_n$; ξ_1 = damping coefficient of passive spring (A value of 0.05 was used for ξ_1.)

$$\text{Active:}\quad \omega_n = \sqrt{\frac{K_{eq}}{M}}\ ;\ \frac{C_{eq}}{M} = 2\xi\omega_n$$

Electromagnitic Damping Effectiveness

$$\left|\bar{X}_f\left[\frac{j\omega}{\omega_n}\right]_v\right| = \sqrt{\frac{\left[1-\left[\frac{\omega}{\omega_n}\right]^2\right]^2 + \left[2\xi_1\frac{\omega}{\omega_n}\right]^2}{\left[1-\left[\frac{\omega}{\omega_n}\right]^2\right]^2 + \left[2\xi\frac{\omega}{\omega_n}\right]^2}} \qquad (17)$$

Where:

$$\frac{c}{M} = 2\xi\omega_n,\ \omega_n = \sqrt{\frac{K}{M}},\ \xi = \frac{1}{2}G_v\sqrt{\frac{1}{KM}}$$

ξ_1 = damping coefficient of passive spring (A value of 0.05 was used for ξ_1.)

These effectiveness functions are plotted in Figs. 6 and 7. Figures 6 and 7 present the effectiveness of the active feedback, force actuated vibration isolation systems as compared to a passive system with a critical damping coefficient of 0.05, which is typical of passive systems of the type utilized with low frequency system resonances.

CONCLUDING REMARKS

In conclusion, it is apparent that the active magnetic systems described here have advantages over passive isolators due to their ability to isolate against the low frequency regime of the orbital carriers, as well as their ability to implement an adaptive control to isolate against both the direct and base excitations which will be present in all pressurized modules. Therefore, the optimal isolation of a microgravity science payload will eventually need an adaptive digitally controlled system in order to optimize isolation coefficients to most effectively prevent disturbances from perturbing the isolated payload. In order to lower the corner frequencies of such an active system one would need to use actuators with larger and larger strokes. However, this would be impossible due to the volume constraints present in space flight vehicles. Thus, such an isolated payload will have to follow these very low steady-state accelerations such as aerodynamic drag and gravity gradient effects. In order to achieve the microgravity requirements imposed on the Space Station facility (Fig. 8), for any significant length of time, microgravity vibration isolation will have to become a systems engineered solution as well as an experiment specific concern. Thus, these requirements for acceleration sensitive microgravity space experiments will dictate multi-stage isolation concepts which will combine both passive and active systems where the control of the center of gravity of the Space Station will be closed around microgravity steady-state accelerations.

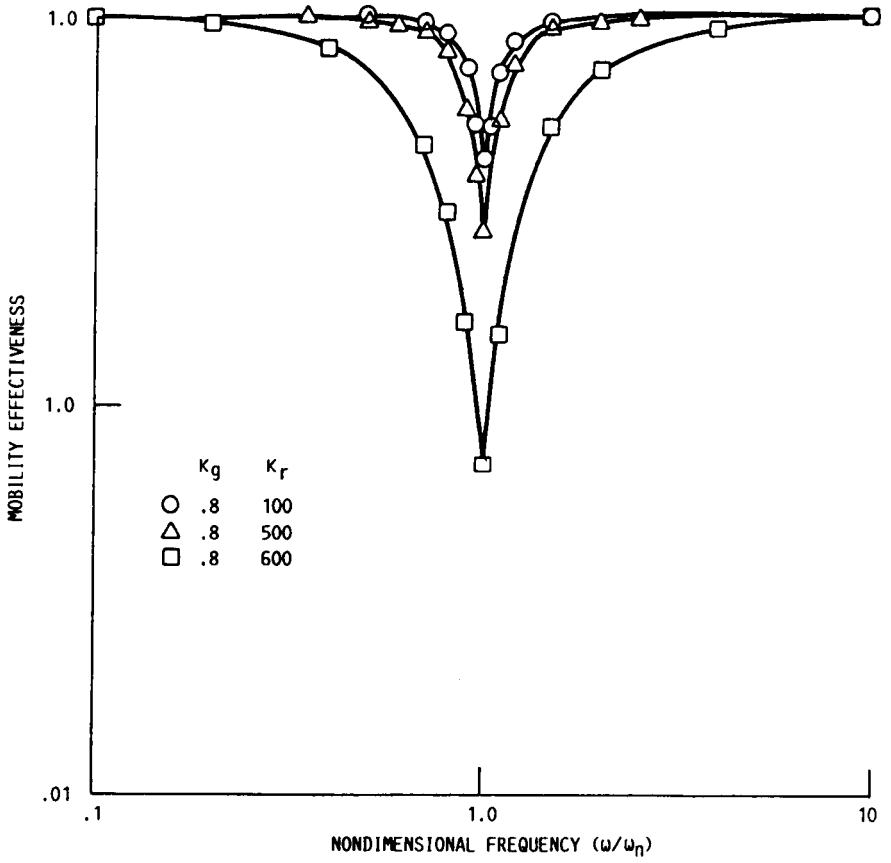

FIGURE 6.

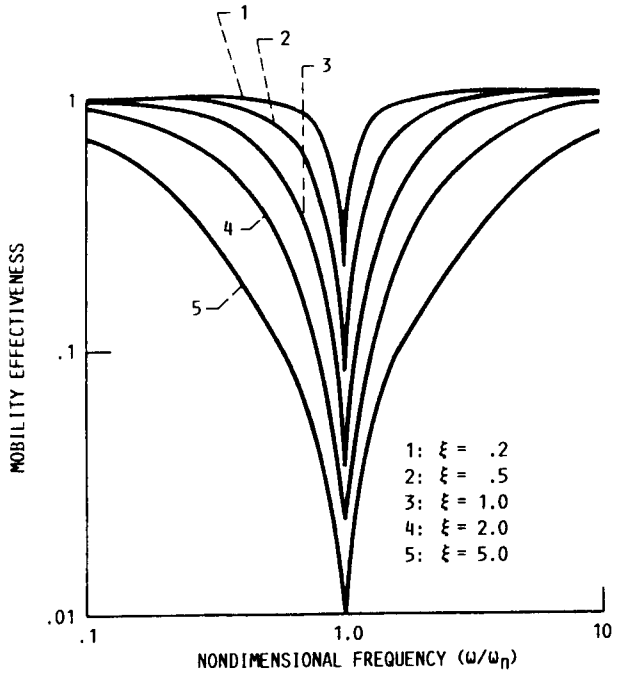

FIGURE 7.

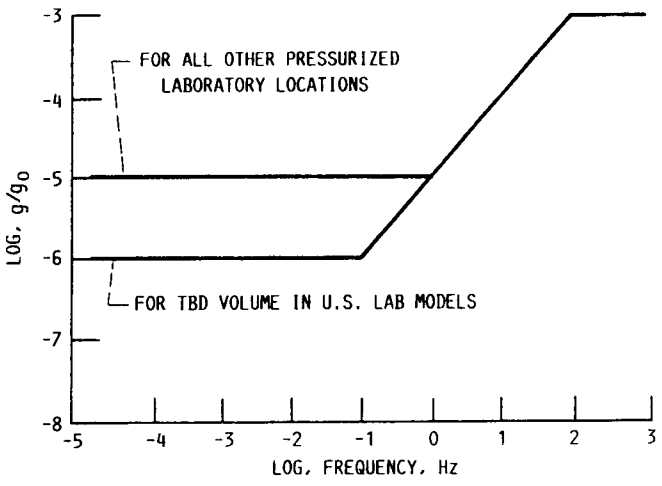

FIGURE 8.

REFERENCES

Grodsinsky, C., 1989, "Development and Approach to Low Frequency Microgravity Isolation Systems," NASA TM, in preparation.

Hamacher, H., 1986, "Simulation of Weightlessness," Materials Sciences in Space, B. Feurbacher, H. Hamacher, and R.J. Naumann, eds., Springer-Verlag, New York, pp. 31-51.

Hamacher, H., Feurbacher, B., and Jilg, R., 1986, "Analysis of Microgravity Measurements in Spacelab," Proceedings of the Fifteenth International Symposium on Space Technology and Science, Vol. 2, H. Matsuo, ed., AGNE Publishing, Tokyo, Japan, pp. 2087-2097.

Humphris, R.R., Kelm, R.D., Lewis, D.W., and Allaire, P.E., 1986, "Effect of Control Algorithms on Magnetic Journal Bearing Properties," Journal of Engineering for Gas Turbines, Vol. 108, No. 4, pp. 624-632.

Jones, D.E., Owens, A.R., Owen, R.G., and Roberts, G., 1987, "Microgravity Isolation Mount," ESA-CR(P)-2480, European Space Agency.

Ruzicka, J.E., 1969, "Active Vibration and Shock Isolation," SAE Paper 680747.

Workshop Proceedings, 1986, "Measurement and Characterization of the Acceleration Environment on Board the Space Station," Guntersville, AL, Aug. 11-14.

APPENDIX

The range of accelerations which have been observed on several STS missions or estimated for the accessible orbit are summarized below (Hamacher, 1986; Ruzicka, 1969; Hamacher, et al., 1986).

Quasi-Steady or "DC" Acceleration Disturbances

g/g_o	Frequency, Hz	Source
10^{-7}	0 to 10^{-3}	Aerodynamic drag
10^{-8}	0 to 10^{-3}	Light pressure
10^{-7}	0 to 10^{-3}	Gravity gradient

Periodic Acceleration Disturbances

g/g_o	Frequency, Hz	Source
$2x10^{-2}$	9	Thruster fire (orbital)
$2x10^{-3}$	5 to 20	Crew motion
$2x10^{-4}$	17	Ku band antenna

Nonperiodic Acceleration Disturbances

g/g_o	Frequency, Hz	Source
10^{-4}	1	Thruster fire (attitude)
10^{-4}	1	Crew push off

NASA
National Aeronautics and Space Administration

Report Documentation Page

1. Report No.	2. Government Accession No.	3. Recipient's Catalog No.
NASA TM-101448		

4. Title and Subtitle

Low Frequency Vibration Isolation Technology for Microgravity Space Experiments

5. Report Date

6. Performing Organization Code

7. Author(s)

Carlos M. Grodsinsky and Gerald V. Brown

8. Performing Organization Report No.

E-4557

10. Work Unit No.

694-03-03

9. Performing Organization Name and Address

National Aeronautics and Space Administration
Lewis Research Center
Cleveland, Ohio 44135-3191

11. Contract or Grant No.

13. Type of Report and Period Covered

Technical Memorandum

12. Sponsoring Agency Name and Address

National Aeronautics and Space Administration
Washington, D.C. 20546-0001

14. Sponsoring Agency Code

15. Supplementary Notes

Prepared for the 12th Biennial Conference on Mechanical Vibration and Noise, sponsored by the American Society of Mechanical Engineers, Montreal, Canada, September 17-20, 1989.

16. Abstract

The dynamic acceleration environment observed on Space Shuttle flights to date and predicted for the Space Station has complicated the analysis of prior microgravity experiments and prompted concern for the viability of proposed space experiments requiring long-term, low-g environments. Isolation systems capable of providing significant improvements in this environment exist, but have not been demonstrated in flight configurations. This paper presents a summary of the theoretical evaluation for two one degree-of-freedom (DOF) active magnetic isolators and their predicted response to both direct and base excitations, that can be used to isolate acceleration sensitive microgravity space experiments.

17. Key Words (Suggested by Author(s))	18. Distribution Statement
Vibration isolators; Vibration damping; Microgravity experiments; Active, Adaptive control; Electromagnetics	Unclassified – Unlimited Subject Category 31

19. Security Classif. (of this report)	20. Security Classif. (of this page)	21. No of pages	22. Price*
Unclassified	Unclassified	9	A02

*For sale by the National Technical Information Service, Springfield, Virginia 22161